Self-Assembled Monolayers of Aromatic Thiols Stabilized by Parallel-Displaced $\pi-\pi$ Stacking Interactions

Rui-Fen Dou,[†,‡] Xu-Cun Ma,[‡] Luan Xi,[†] Hin Lap Yip,[†] King Young Wong,[†] Woon Ming Lau,[†] Jin-Feng Jia,[‡] Qi-Kun Xue,*[,‡] Wei-Sheng Yang,[§] Hong Ma,[||] and Alex K-Y. Jen[||]

Department of Physics and Materials Science and Technology Research Centre, The Chinese University of Hong Kong, Shatin, Hong Kong, China, State Key Laboratory for Surface Physics, Institute of Physics, Chinese Academy of Sciences, Beijing 100080, China, Department of Physics, Peking University, Beijing 100871, China, and Department of Materials Science and Engineering, University of Washington, Seattle, Washington 98195

Received November 7, 2005

Parallel-displaced $\pi-\pi$ stacking interactions have been known to be the dominant force in stabilizing the double helical structure of DNA and the tertiary structure of proteins. However, little is known about their roles in self-assembled monolayers of other large π molecules such as aromatic thiols. Here we report on a systematic study of the self-assembled monolayers of four kinds of anthracene-based thiols, 9-mercaptoanthracene (MA), (4-mercaptophenyl) (9-anthryl) acetylene (MPAA), (4-mercaptophenyl) (10-nitro-9-anthryl) acetylene (MPNAA), and (4-mercaptophenyl) (10-carboxyl-9-anthryl) acetylene (MPCAA) on Au(111), in which a spacer and different functional groups (NO_2 and COOH) are intentionally designed to introduce and thus allow the investigation of various intermolecular interactions, in addition to $\pi-\pi$ interactions in the base molecules. We find that all molecules form long-range-ordered monolayers and, more interestingly, that these assembled monolayers exhibit essentially the same fundamental packing structure. On the basis of high-resolution scanning tunneling microscopy observations, we propose the space-filling models for the observed superstructures and demonstrate that all superstructures can be understood in terms of the parallel-displaced $\pi-\pi$ stacking interactions, despite the presence of competing dipole−dipole and H-bonding interactions associated with these specially designed functional groups.

Introduction

Thiols on Au(111) is a model system for the investigation of self-assembled monolayers (SAMs),[1] whereas *n*-alkyl thiols are considered to be the simplest and an archetypal case among them and have been studied the most.[2] As a result, the general behavior of such relatively simple model systems in terms of the molecular packing, the appearance of various phases during growth, and how the molecular features affect the structure and growth behavior is now relatively well understood within certain limits.[2]

More recently, these efforts have been extended to SAMs of aromatic thiols[3−17] because of a number of important applications such as charge-transfer control,[18] organic electronics,[19,20] and nanometer-scale patterning.[21,22] It is generally believed that in the SAMs of complex organic molecules the delicate balance between intermolecular and adsorbate−substrate interactions determines their structure and packing characteristics[1,2] and that the intermolecular interactions as well as the steric constrains largely depend on the molecular features, for example, the backbones and tail groups. In this respect, the key difference between the aliphatic and aromatic thiols is the rigid π character of the latter, which makes SAMs of these two kinds of thiols

* To whom correspondence should be addressed. E-mail: qkxue@aphy.iphy.ac.cn.

[†] The Chinese University of Hong Kong.

[‡] Chinese Academy of Sciences.

[§] Peking University.

[||] University of Washington.

(1) Ulman, A. *Chem. Rev.* **1996**, *96*, 1533−1554.

(2) Schreiber, F. *Prog. Surf. Sci.* **2001**, *65*, 151−256.

(3) Wan, L. J.; Terashima, M.; Noda, H.; Osawa, M. *J. Phys. Chem. B* **2000**, *104*, 3563−3569. Jin, Q.; Rodriguez, J. A.; Li, C. Z.; Darici, Y.; Tao, N. J. *Surf. Sci.* **1999**, *425*, 101−111.

(4) Leung, T. Y. B.; Schwartz, P.; Scoles, G.; Schreiber, F.; Ulman, A. *Surf. Sci.* **2000**, *458*, 34−52.

(5) Kang, J. F.; Ulman, A.; Liao, S.; Jordan, R.; Yang, G. H.; Liu, G. Y. *Langmuir* **2001**, *17*, 95−106. Cyganik, P.; Buck, M.; Azzam, W.; Wo1l, *C. J. Phys. Chem. B* **2004**, *108*, 4989−4996.

(6) Rong, H. T.; Frey, S.; Yang, Y. J.; Zharnikov, M.; Buck, M.; Wuhn, M.; Woll, C.; Helmchen, G. *Langmuir* **2001**, *17*, 1582−1593.

(7) Ulman, A. *Acc. Chem. Res.* **2001**, *34*, 855−863.

(8) Cyganik, P.; Buck, M. *J. Am. Chem. Soc.* **2004**, *126*, 5960−5961.

(9) Dhirani, A. A.; Zehner, R. W.; Hsung, R. P.; Guyot-Sionnest, P.; Sita, L. R. *J. Am. Chem. Soc.* **1996**, *118*, 3319−3320.

(10) Tao, Y. T.; Wu, C. C.; Eu, J. Y.; Lin, W. L. *Langmuir* **1997**, *13*, 4018−4023.

(11) Yang, G. H.; Qian, Y.; Engtrakul, C.; Sita, L. R.; Liu, G. Y. *J. Phys. Chem. B* **2000**, *104*, 9059−9062.

(12) Garg, N.; Carrasquillo-Molina, E.; Lee, T. R. *Langmuir* **2002**, *18*, 2717−2726.

(13) Azzam, W.; Wehner, B. I.; Fischer, R. A.; Terfort, A.; Woll, C. *Langmuir* **2002**, *18*, 7766−7769.

(14) Walzer, K.; Marx, E.; Greenham, N. C.; Less, R. J.; Raithby, P. R.; Stokbro, K. *J. Am. Chem. Soc.* **2004**, *126*, 1229−1234.

(15) Krings, N.; Strehblow, H.-H.; Kohnert, J.; Martin, H.-D. *Electrochim. Acta* **2003**, *49*, 167−174.

(16) Imahori, H.; Norieda, H.; Nishimura, Y.; Yamazaki, I.; Higuchi, K.; Kato, N.; Motohiro, T.; Yamada, H.; Tamaki, K.; Arimura, M.; Sakata, Y. *J. Phys. Chem. B* **2000**, *104*, 1253−1260.

(17) Yasseri, A. A.; Syomin, D.; Malinovskii, V. L.; Loewe, R. S.; Lindsey, J. S.; Zaera, F.; Bocian, D. F. *J. Am. Chem. Soc.* **2004**, *126*, 11944−11953.

(18) Adams, D. M.; Brus, L.; Chidsey, C. E. D.; Creager, S.; Creutz, C.; Kagan, C. R.; Kamat, P. V.; Lieberman, M.; Lindsay, S.; Marcus, R. A.; Metzger, R. M.; Michel-Beyerle, M. E.; Miller, J. R.; Newton, M. D.; Rolison, D. R.; Sankey, O.; Schanze, K. S.; Yardley, J.; Zhu, X. *J. Phys. Chem. B* **2003**, *107*, 6668−6697.

(19) Donhauser, Z. J.; Mantooth, B. A.; Kelly, K. F.; Bumm, L. A.; Monnell, J. D.; Stapleton, J. J.; Price, D. W.; Rawlett, A. M.; Allara, D. L.; Tour, J. M.; Weiss, P. S. *Science* **2001**, *292*, 2303−2307.

(20) Li, C.; Zhang, D. H.; Liu, X. L.; Han, S.; Tang, T.; Zhou, C. W.; Fan, W.; Koehne, J.; Han, J.; Meyyappan, M.; Rawlett, A. M.; Price, D. W.; Tour, J. M. *Appl. Phys. Lett.* **2003**, *82*, 645−647.

(21) Xia, Y. N.; Rogers, J. A.; Paul, K. E.; Whitesides, G. M. *Chem. Rev.* **1999**, *99*, 1823−1848.

(22) Gölzhäuser, A.; Eck, W.; Geyer, W.; Stadler, V.; Weimann, T.; Hinze, P.; Grunze, M. *Adv. Mater.* **2001**, *13*, 806−809.

10.1021/la052987u CCC: $33.50
Published on Web 03/03/2006

Chart 1

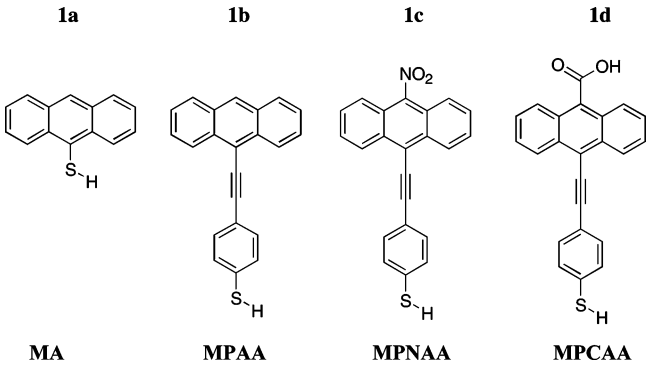

significantly different from each other.[7] Moreover, it has been shown that in the aliphatic SAMs the headgroup−substrate interaction is a decisive factor, whereas in aromatic SAMs such as biphenyl−thiol (BPT) and terphenyl−thiol (TPT) the structure and packing of the molecules are mainly determined by the intermolecular interactions.[23] Therefore, research on SAMs of aromatic thiols has an impact on both science and technology, but it is still an emerging and challenging subject.

Intermolecular interactions in SAMs of aromatic thiols are rather complicated.[3−17] Two aspects in these recent studies are particularly noted.[3−15] First, the aromatic molecules studied [2] were mostly based on benzene,[3] biphenyl,[4−8] oligophenyl,[9−13] and oligophenylethynyl thiols,[14] but only a few of them are aromatic molecules with a rigid, large π-system.[15−17] Second, the herringbone-shaped structure seems to be the most common structure convincingly measured from these thiol molecules, and the importance of T-shaped $\pi-\pi$ interactions has overshadowed that of parallel-displaced interactions.[5−7,9,11] However, the importance of parallel-displaced $\pi-\pi$ interactions is bound to rise with an increase in aromatic molecule size. In fact, it is well known that the parallel-displaced $\pi-\pi$ interactions are the most important interactions in stabilizing the double helical structure of DNA[24,25] and the tertiary structures of proteins.[24,26] In crystals of aromatic molecules, the parallel-displaced $\pi-\pi$ interactions dominate the majority of the structures and account for over 50% of the total lattice energy and are also the most important interactions.[24,27] To explore the roles of parallel-displaced $\pi-\pi$ interactions in the self-assembly process of aromatic thiols, we have designed and synthesized four anthracene-based aromatic thiols with rigid, large π-systems (i.e., 9-mercaptoanthracene (MA), (4-mercaptophenyl) (9-anthryl) acetylene (MPAA), (4-mercaptophenyl) (10-nitro-9-anthryl) acetylene (MPNAA), and (4-mercaptophenyl) (10-carboxyl-9-anthryl) acetylene (MPCAA)) (Chart 1). By attaching different functional groups onto the base MPAA molecule, various interactions can be investigated in a well-controlled and systematic manner. In this article, we report our scanning tunneling microscopy study of the self-assembled monolayers of these four specially designed molecules with the aim of clarifying the roles of the parallel-displaced $\pi-\pi$ interactions.

The principal design considerations of these four molecules are as follows. (i) To ensure that the dominant intermolecular interactions in the SAMs are parallel-displaced $\pi-\pi$ interactions, an anthryl group is included in all four types of molecules because recent ab initio calculations have shown that that larger π-systems prefer parallel-displaced rather than T-shaped $\pi-\pi$ interactions and that the larger the π-systems the stronger the parallel-displaced $\pi-\pi$ interactions.[28] (ii) To make the $\pi-\pi$ interactions truly parallel-displaced, the long in-plane axis of the anthryl group is placed horizontally instead of vertically for T-shaped $\pi-\pi$ interactions,[15] and the thiol group is directly connected to the center 9-position of the anthryl group in the case of MA. (iii) Because a spacer, especially a long one, may improve the long-range ordering of the SAMs,[5,9,16] a phenyl-acetylene group is inserted as a spacer between the anthryl and the thiol groups in the case of MPAA. (iv) To facilitate a broad range of applications, functional groups are also included as part of the headgroup, backbone, and end group on the molecules.[2,7] In general, functional groups affect the intermolecular interactions and thus modify or even completely change the structure of the SAMs. To determine whether the rigidity of parallel-displaced $\pi-\pi$ interactions will stabilize SAMs of large π-systems against other intermolecular interactions, the structures of SAMs of MPNAA and MPCAA, in which NO_2 and COOH functional groups are attached to MPAA, respectively, are also studied.

Experimental Section

The Au(111) substrates used in our experiment were bought from Molecular Image. The received gold substrates were annealed in the butane flame, and after cooling, they were immersed in 50 μM dilute ethanol solutions of MA, MPAA, MPNAA, and MPCAA, respectively, at room temperature. These solutions containing the gold substrates were conserved in a sealed vessel filled with high-purity nitrogen gas (N_2) for a certain time interval to form the SAMs. The SAM samples were subsequently rinsed thoroughly with ethanol and finally dried under N_2 flow. Then the samples were transferred to the UHV chamber for STM study. The STM experiments were performed in a commercial Omicron ultrahigh-vacuum STM system. All STM images shown here were recorded at room temperature in constant current mode using a Pt−Ir tip prepared by ac chemical etching. The tunneling current was set between 10 and 80 pA, and the tip bias voltage was varied from −1.7 V to +1.7 V with the grounded sample.

Results and Discussion

1. Self-Assembly of MA Molecules. We first studied the adsorption of the simplest MA (Chart 1a) molecules on the Au(111) substrate. The STM images shown in Figure 1 were obtained from the sample prepared by immersing the Au(111) substrate in a dilute solution of MA for 24 h. As one can see from Figure 1a, the surface is covered with different domains of ordered structures. Although certain small domains are only about 50 Å in size, the bright protrusions in each domain are well ordered with few defects (Figure 1b). The average area of a protrusion is $S = b \sin \alpha(^a/_4) = 55$ Å^2, where a, b, and α are the lengths of the two unit vectors and the angle between them, respectively (Figure 1b). Because S is quite close to the van der Waals area of a single standing-up anthryl group ($\sim$52 Å^2), we believe that each protrusion corresponds to a standing-up MA molecule. Actually, aromatic thiolates, at least at high coverage, tend to take the standing-up conformation on Au substrates,[5−17] and every molecule can usually be imaged as a protrusion with STM.[5,9,11] A careful inspection of Figure 1b indicates that the molecules are aligned into wavelike rather than straight rows, with a period of four molecules. In the close-up image (Figure

(23) Zharnikov, M.; Grunze, M. *J. Phys.: Condens. Matter* **2001**, *13*, 11333−11365.
(24) Hunter, C. A.; Sanders, J. K. M. *J. Am. Chem. Soc.* **1990**, *112*, 5525−5534.
(25) Saenger, W. *Principles of Nucleic Acid Structure*; Springer-Verlag: New York, 1984; pp 261−265.
(26) McGaughey, G. B.; Gagné, M.; Rappé, A. K. *J. Biol. Chem.* **1998**, *273*, 15458−15463.
(27) Thetford, D.; Cherryman, J.; Chorlton, A. P.; Docherty, R. *Dyes Pigm.* **2004**, *63*, 259−276.
(28) Lee, N. K.; Park, S.; Kim, S. K. *J. Chem. Phys.* **2000**, *116*, 7902−7909. Lee, N. K.; Park, S.; Kim, S. K. *J. Chem. Phys.* **2000**, *116*, 7910−7917.

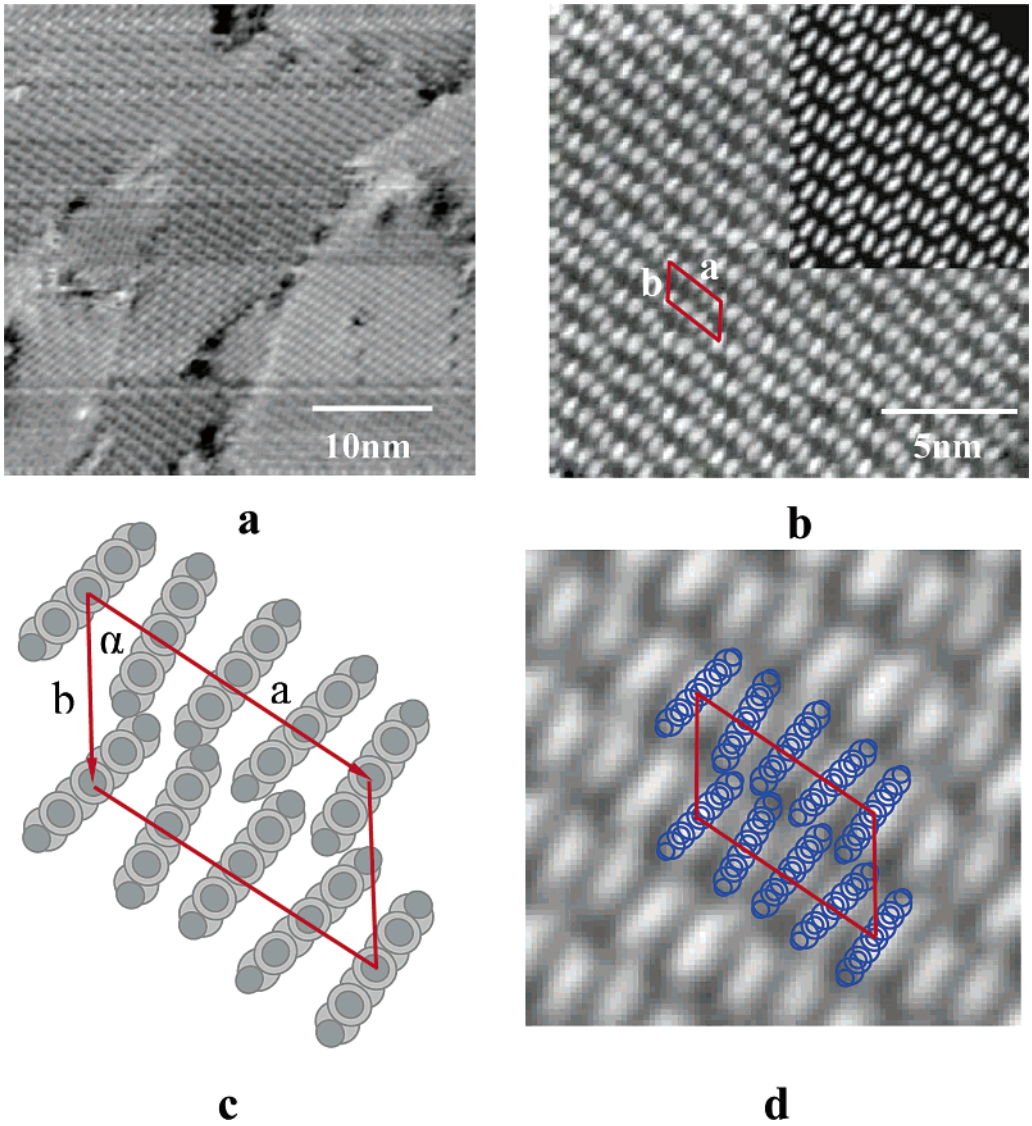

Figure 1. (a) STM image of the MA SAM on Au(111) showing multidomain structures (V_{sample} = 1.2 V, I_t = 0.07 nA). (b) Typical molecular-resolution STM image of the MA SAM with periodical superstructures (V_{sample} = 1.4 V, I_t = 0.06 nA). A unit cell of the superstructure is outlined by a solid parallelogram, where **a**, **b**, and α are approximately 22.5 Å, 12.7 Å, and 51°, respectively. The upper-right inset is the simulated STM image based on the proposed model. (c) Schematic drawing of the model proposed for the ordered structure of MA/Au(111). (d) Structural model overlaid on a high-resolution STM image.

1d), one even finds that each molecule looks like a bar and that the neighboring bars are not precisely parallel to each other but form small angles. Because the MA molecules are in a standing-up conformation and have no functional group but the anthryl group, one would not be surprised to see an anthracene imaged as a bar lying along its long axis.

A model has been proposed for the molecular arrangement in the SAM of MA and is schematically shown in Figure 1c. To show that the model really accounts for the structure of the SAM, we superimpose the model on the image in Figure 1d, and a patch of the simulated image is shown in the upper-right corner of Figure 1b. Note that the image was simulated from the model by assuming that in large-scale images each MA molecule corresponds to an oval feature located at its central anthryl group. As one can see from these Figures, the model reflects the major features of the SAM quite well. If we recall the packing characteristic of two benzene molecules aligning into a parallel-displaced dimer, then on the basis of the above model, we deduce that the dominant intermolecular interactions in the MA SAM should be parallel-displaced $\pi-\pi$ stacking interactions along the direction of the wavelike rows. To compromise the parallel-displaced $\pi-\pi$ stacking interactions and steric constraint, the neighboring anthryl groups have to be tilted a bit. In the model, it is noted that the center−center separation R_{CEN},[26] the parallel-displacement angle θ,[26] and the tilt angle γ [26] of the neighboring anthracene groups are approximately 5.6 Å, 10°, and 12°, respectively. Compared with the data obtained for proteins,[26] these values are quite reasonable. As for why R_{CEN} is a little large compared to the ab initio calculations,[28] we recall that the calculations were performed for free-standing molecules (π-systems), whereas the adsorbate−substrate interaction is also involved in the present cases.

2. Self-Assembly of MPAA Molecules. As mentioned above, MPAA (Chart 1b) was expected to form similar structure but with better ordering, compared with MA. The STM images of our MPAA/Au(111) sample confirm this expectation. As shown in Figure 2a, one can see that the MPAA molecules indeed self-assemble into wavelike rows similar to those of MA with a period of four molecules, probably with a slightly smaller amplitude change according to the image contrast. For the MA SAMs, the domain sizes are small, often with some defects. In the case of MPAA, the domains expand over tens of nanometers,

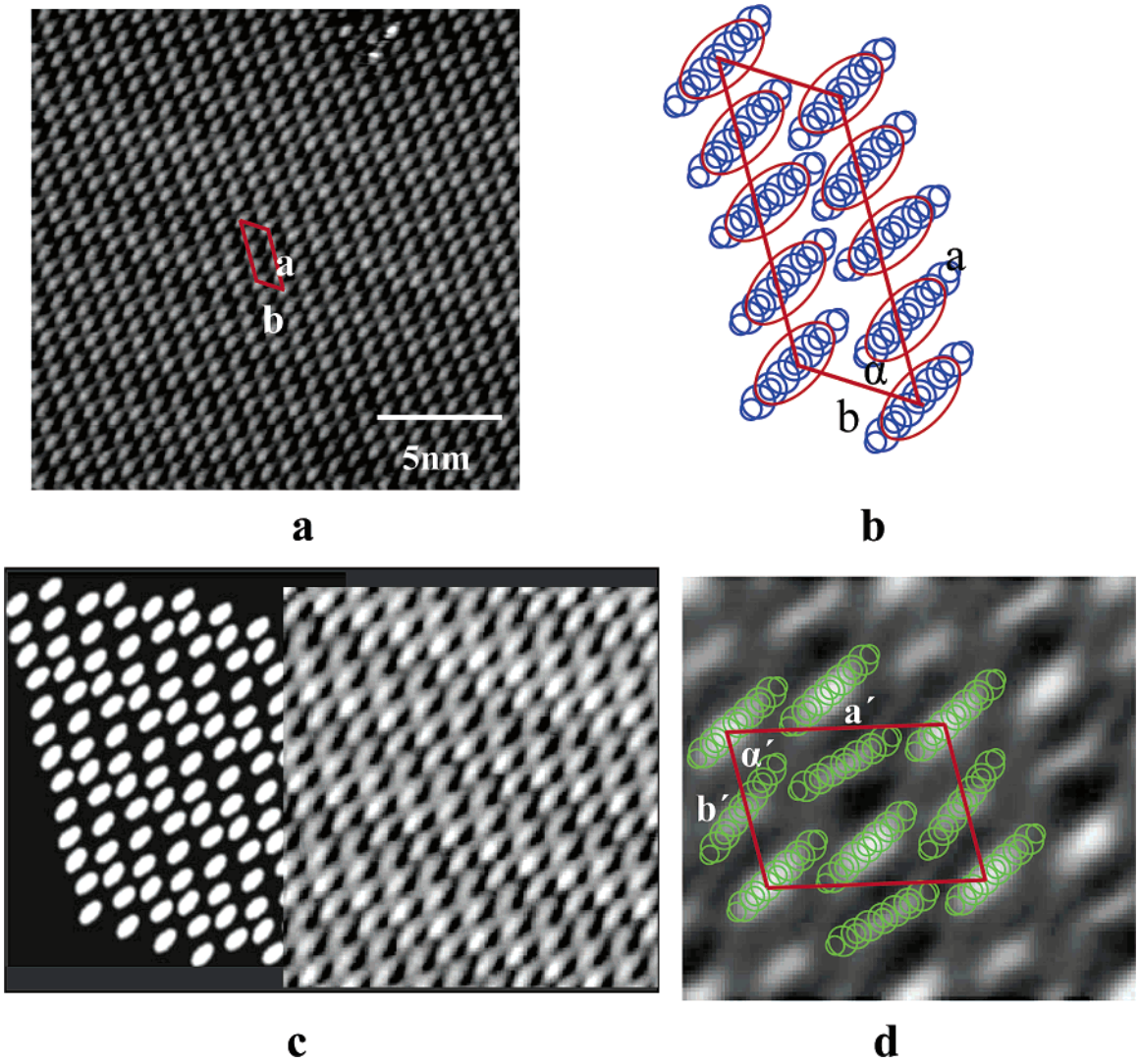

Figure 2. (a) Molecular-resolution STM image of the MPAA SAM on Au(111) showing well-ordered structures ($V_{sample} = -0.8$ V, $I_t = 0.05$ nA). A unit cell of the superstructure is outlined by a solid parallelogram, where **a**, **b**, and α are approximately 25.6 Å, 9.9 Å, and 57°, respectively. (b) Schematic drawing of the model proposed for the ordered structure of MPAA/Au(111). (c) Corresponding relationship between the simulated STM image based on the proposed model and the experimental STM image. (d) STM image of another ordered superstructure observed in the same sample surface ($V_{sample} = -0.6$ V, $I_t = 0.05$ nA). Two unit vectors (**a′** and **b′**) and the angle (α′) between them are approximately 18.3 Å, 12.0 Å, and 76°, respectively.

and almost no defects are observed. We believe that this is due to the inclusion of the phenyl-acetylene spacer in MPAA. The flexibility of the molecules can more easily coordinate the steric constraint and different interactions, as required for molecular ordering, and thereby makes larger ordered domains and fewer defects.

The average area of a protrusion is approximate 53 Å^2, which is slightly smaller than 55 Å^2 for MA, suggesting that each protrusion is the image of a standing-up MPAA molecule. With the same consideration, a model is proposed for the molecular arrangement and is schematically shown in Figure 2b. The simulated image shown beside the STM image in Figure 2c does account for the SAM structure. The intermolecular part of the driving force for this structure must also be the parallel-displaced $\pi-\pi$ stacking interactions in the direction of the wavelike molecular rows, and R_{CEN}, θ, and γ are about 6.4 Å, 30°, and 10°, respectively. Despite the similarity between MA and MPAA, there is still a significant quantitative difference in terms of $P = b \sin \alpha/(a/4) = d_{\text{inter}-\pi \text{ row}}/d_{\text{intra}-\pi \text{ row}}$, where $d_{\text{inter}-\pi \text{ row}}$ is the mean separation between neighboring molecules in two neighboring rows and $d_{\text{intra}-\pi \text{ row}}$ is the mean separation between neighboring molecules in a $\pi-\pi$ row. The measured values of P are 1.76 and 1.29 for MA and MPAA, respectively. This difference is, very likely, also a result of the higher flexibility of MPAA molecules, which enables molecules to yield to satisfy the requirements for molecular packing in neighboring rows. As a result, the SAM of MPAA has a smaller S than that for MA.

It is noteworthy that another SAM structure of MPAA was also observed that coexists with the above structure on the surface. This is quite understandable because molecules with higher flexibility are more tolerable in terms of both intermolecular and adsorbate−substrate interactions and allow slightly different structures to form. The two structures have almost identical R_{CEN}, θ, γ, and P values and thus must be driven by the same intermolecular interactions. Thus, further discussion is not necessary, and we give only an enlarged image with the proposed model in Figure 2d.

3. Self-Assembly of MPNAA Molecules. To check the stability of the SAMs of MPAA against different functional groups and thus interacting mechanisms, we start with MPNAA, which has a NO_2 group (Chart 1c). We find not only that MPNAA molecules can self-assemble into the well-ordered SAM with domains as large as 500 Å but also that they exhibit structures that are extremely similar to those of the former two systems. The observed

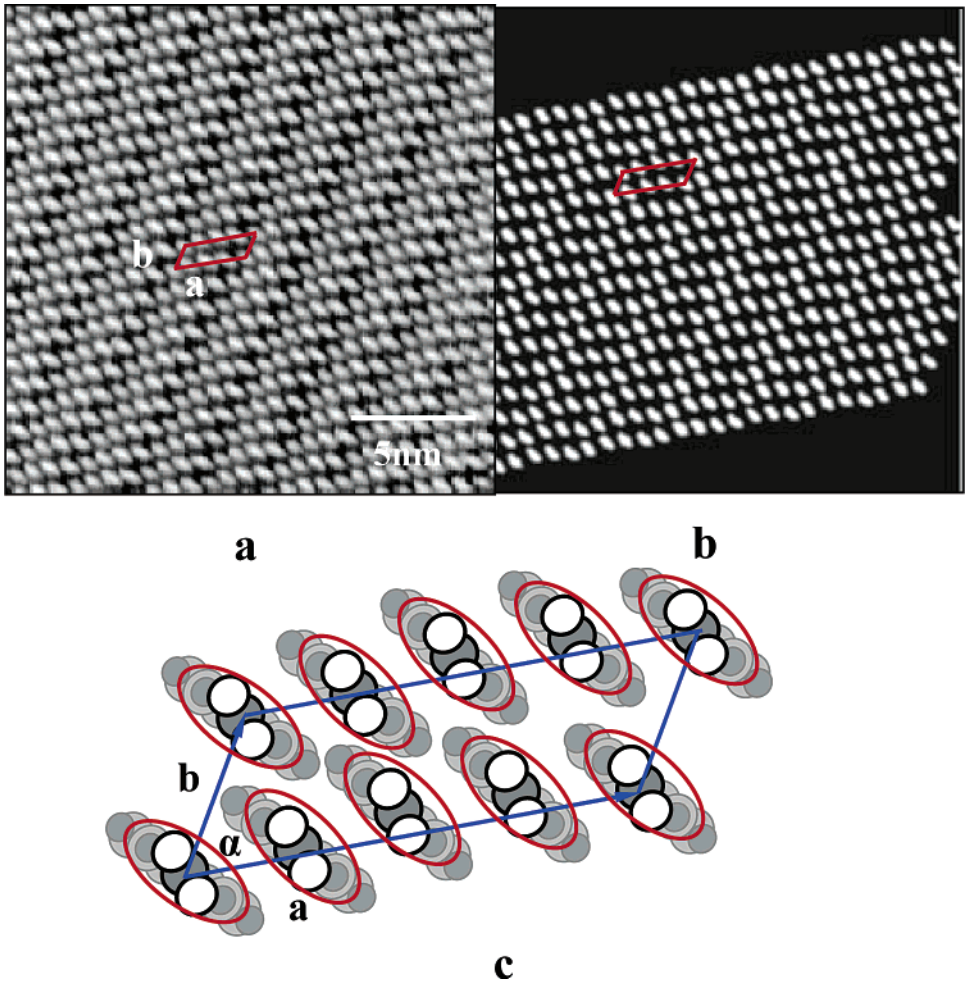

Figure 3. (a) Molecular-resolution STM image of the well-ordered MPNAA SAM on Au(111) ($V_{sample} = +0.4$ V, $I_t = 0.04$ nA). (b) Simulated large-area STM image based on the proposed model shown in c. Two dashed parallelograms in a and b indicate the unit cell of the superstructure. Two unit vectors (**a** and **b**) and the angle (α) between them in a are about 28.0 Å, 9.8 Å, and 56°, respectively. (c) Schematic drawing of the structural model proposed for MPNAA/Au(111).

and simulated STM images with the wavelike row structure with four molecules in a unit cell are shown in Figure 3a and b, respectively, which agree with each other very nicely. Because MPNAA has a NO_2 group attached to the anthryl group, in general it would be difficult to identify the orientations of the anthryl groups directly from the STM images, unlike what we did for the previous two systems. Consequently, to propose the model, we have to consider the van der Waals dimensions of the molecules in addition to those required for the $\pi-\pi$ stacking interactions. The rest of the considerations in the model are the same as those mentioned above. The model is shown in Figure 3c.

The NO_2 group induces two differences compared to the SAMs above, as for the mercaptobiphenyl SAMs studied previously.[7] One is in the adsorption kinetics: the well-developed SAM of MPNAA appear only if the substrates are kept in the solution for 48 h or longer, whereas for the previous two systems 24 h is enough, indicating that the NO_2 group significantly slows down the self-assembly process. Actually, for the SAMs of aromatic 4-mercaptobiphenyls,[7] it has been shown that different electron-withdrawing substituents at the 4′ position lead to molecular dipole moments that are due to the asymmetric electron distribution between the electron-withdrawing group ($-NO_2$) and the electron-donating group (the thiolate). The resulting dipole−dipole interactions introduce a nucleation barrier that slows down the self-assembly process of the adsorbates on Au substrates.[7] The other one is in the equilibrium structure: the SAM structure of MPNAA has a reduced $d_{inter-\pi\ row}$ and an enlarged $d_{intra-\pi\ row}$ compared with those for MPAA ($P = 1.16$, smaller than 1.29 for MPAA). In addition, for the SAM structure of MPNAA, S is 57 Å^2/molecule, larger than 53 Å^2/molecule for MPAA. We believe that these quantitative changes are also a result of the molecular dipole moments because the NO_2 group introduces the dipole−dipole repulsive intermolecular interactions along the $\pi-\pi$ rows, which increase the separations of the molecules but not the relative orientations. In this case, a more homogeneous but slightly looser molecular arrangement would be energetically more favorable for MPNAA.

4. Self-Assembly of MPCAA Molecules. Because of potential applications of the SAMs with a carboxyl group,[29] the last system we studied is MPCAA (Chart 1d) on Au(111). After immersing the substrate in a dilute solution of MPCAA for 24 h, a well-developed SAM appeared on the surface. A typical STM image is shown in Figure 4a, from which we see clearly that the MPCAA molecules again self-assemble into the wavelike rows structure with four molecules per unit cell. In other words, the major, common features of the SAM structures discussed above, which are stabilized mainly by $\pi-\pi$ stacking intermolecular interactions, are also preserved in the case of MPCAA regardless of the inclusion of the carboxyl group. To establish the structural model, we must consider H-bonding interactions, in addition to $\pi-\pi$

(29) Himmel, H.-J.; Terfort, A.; Wöll, C. *J. Am. Chem. Soc.* **1998**, *120*, 12069−12074.

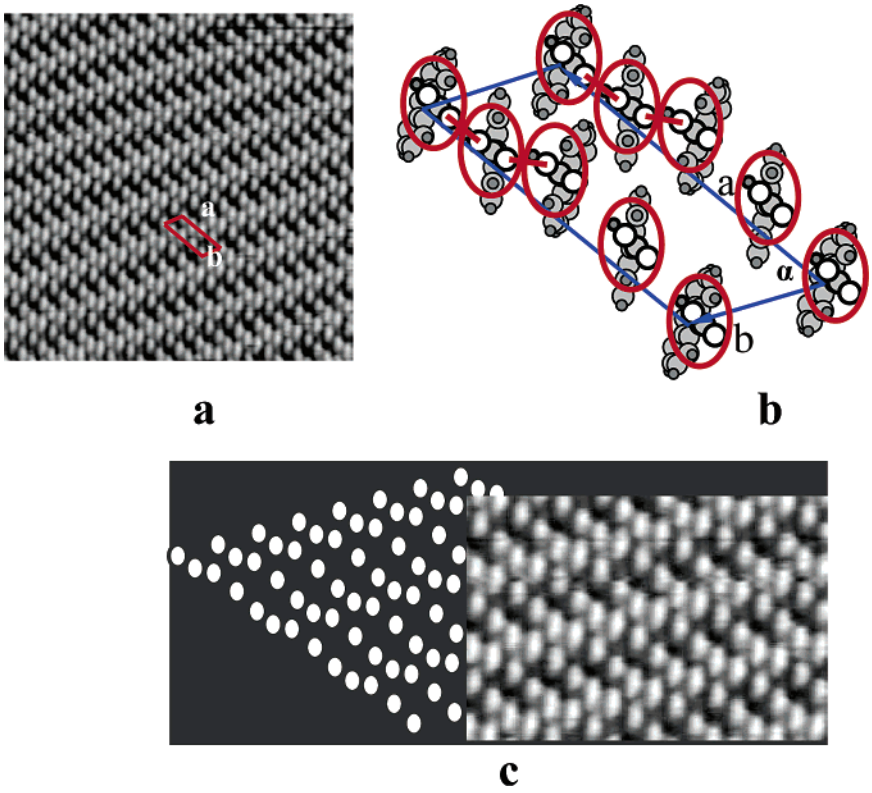

Figure 4. (a) Molecular-resolution STM image of the well-ordered MPCAA SAM on Au(111) for 24 h ($V_{sample} = -0.4$ V, $I_t = 0.04$ nA). A unit cell is outlined by a solid parallelogram, where **a**, **b**, and α are approximately 26.8 Å, 10.8 Å, and 57°, respectively. (b) Schematic drawing of the structural model of MPCAA/Au(111) for 24 h. (c) Simulated large-area STM image (the left panel) and the experimental STM image (the right panel) showing good correspondence between them.

stacking and dipole−dipole intermolecular interactions, because of the hydrogen bonds associated with −COOH••HOOC− in this system. H-bonding interactions have been known to play important roles in the formation of many organic SAMs.[29−31] The model thus proposed is schematically shown in Figure 4b, where three of every four molecules along a $\pi-\pi$ row in a unit cell form a trimer bonded together by two hydrogen bonds with a normal length of about 3 Å, leaving the fourth far away from the trimer. Similar to the MPNAA case, MPCAA also has a functional group (i.e., the carboxyl group) on top, and thus it would be also difficult to resolve the orientations of the anthryl groups directly from the STM images. Consequently, to understand the model, we still have to consider the van der Waals dimensions of the molecules, including their carboxyl groups and anthryl groups, along with all intermolecular interactions. From the simulated image in Figure 4c, we see that the model explains the major features of the STM images well: the wavelike feature and especially the trimer−monomer feature along the $\pi-\pi$ rows, which results from H-bonding. Compared to the SAM structures discussed above, here the $\pi-\pi$ stacking interactions are not satisfied. This is reasonable when we recall the fact that hydrogen bonds have very large formation energies.[32] The presence of hydrogen bonds in this SAM structure is able to compensate for the energy loss due to not only the slightly larger S (60 Å^2/molecule) but also the $\pi-\pi$ stacking interactions that are not satisfied.

Despite the fact that the SAM in Figure 4a looks almost perfect in every sense, we find that, surprisingly, MPCAA molecules can self-assemble into a completely different structure if we only increase the assembling time. Figure 5a shows an STM image from the sample immersed in the same dilute MPCAA solution for 48 h. The new SAM (i.e., the 48 h SAM) appears to be very ordered. Although the structure of this SAM also consists of wavelike rows with a period of four molecules, lying horizontally in Figure 5a, we believe that the driving force is qualitatively different from that for the 24 h one as well as for all of those mentioned above. If a similar mechanism is considered, then the amplitude modulation (∼11 Å) in the wave would be too large to be compatible with that allowed for the parallel-displaced $\pi-\pi$ stacking (3−6 Å).

By carefully studying Figure 5a, we find that the molecules actually form tetramers and that the SAM is made up of periodically arranged tetramers. A plausible model is proposed for further investigation and is schematically shown in Figure 5b. In this structure, every set of four molecules is grouped together by four hydrogen bonds forming a tetramer, and the four tetramers are tilted a bit toward the tetramer center to form hydrogen bonds with the correct bonding length of ∼3 Å. As a result, the $\pi-\pi$ stacking interactions are no longer the parallel-displaced type but are V-shaped for both intra-tetramer and inter-tetramer interactions. The model reproduces well all features seen from the STM images in Figure 5. To simulate the image from the model, we consider that STM mainly images the top-most carboxyl groups of the MPCAA molecules even if the molecules are slightly tilted. In other words, each tetramer of molecules was imaged as a tetramer of protrusions, which are essentially on top of the carboxyl groups, as highlighted by the circles in Figure 5b. As for why the circles are not put precisely above the functional groups but a bit away from the tetramer center, our consideration is that for small clusters, such as the

(30) Zhao, X. Y.; Yan, H.; Zhao, R. G.; Yang, W. S. *Langmuir* **2003**, *19*, 809−813.
(31) Zhao, X. Y.; Zhao, R. G.; Yang, W. S. *Langmuir* **2002**, *18*, 433−438.
(32) Vinogradov, S. N.; Linnell, R. H. *Hydrogen Bonding*; Van Nostrand Reinhold: New York, 1971.

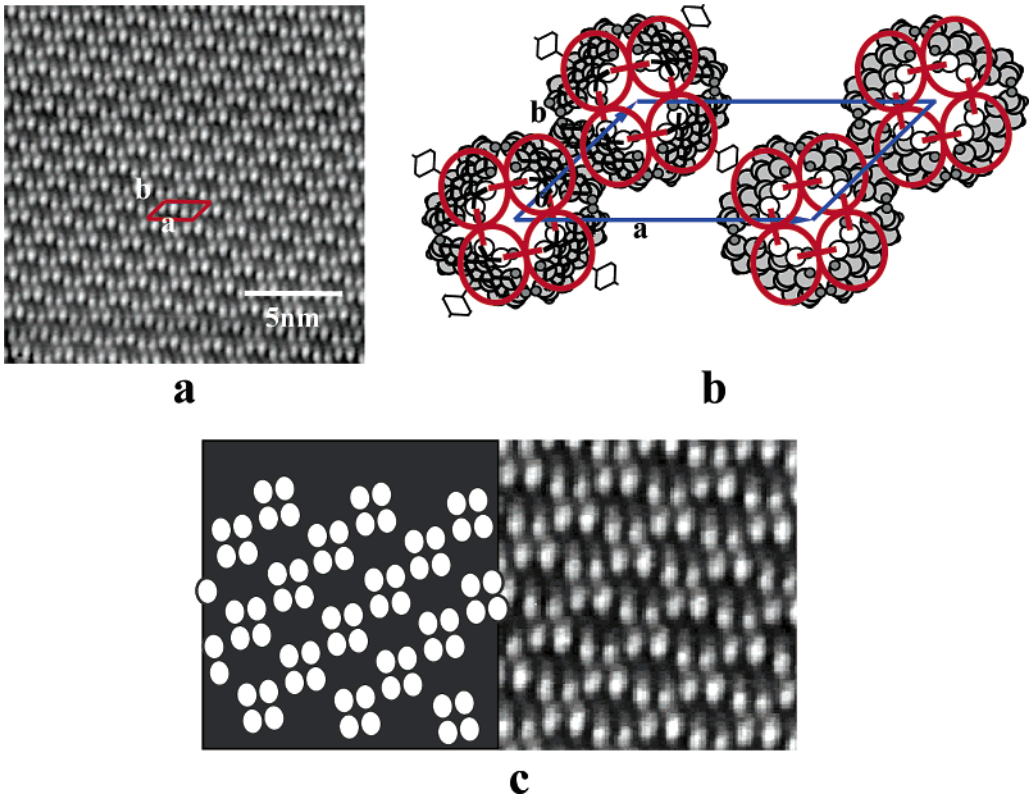

Figure 5. (a) Molecular-resolution STM image of the ordered MPCAA SAM on Au(111) for 48 h ($V_{sample} = -0.8$ V, $I_t = 0.03$ nA). A unit cell is outlined by a solid parallelogram, where **a**, **b**, and α are approximately 24.2 Å, 13.3 Å, and 48°. (b) Schematic drawing of the structural model of MPCAA/Au(111) for 48 h. (c) Simulated (the left panel) and observed STM images corresponding to each other very nicely.

tetramers in the present case, the imaged features are always a bit broadened and off-center because of the STM tip convolution.

Interestingly, the molecular density *S* in the 48 h case is about 60 Å^2/molecule, the same as that in the 24 h SAM, indicating that the increased experimental time for assembly does not change the coverage. The fact that the tetramerlike SAM can form at the expense of the existing wavelike SAM enables us to conclude that the 48 h SAM is a more energetically favorable structure. Considering that in the 48 h SAM each molecule is bonded by 1 H-bond whereas in the 24 h SAM each molecule is bonded on average by only $^1/_2$ H-bond, even if the V-shaped $\pi-\pi$ stacking involved in this structure is less favorable for π-systems,[33] especially for larger π-systems,[24−26] this is still quite understandable. The energy increase from the parallel-displaced to V-shaped $\pi-\pi$ stacking is smaller than the energy reduction due to the formation of an extra two H-bonds per unit cell, and the net energy gain of this phase transition is approximately 278 meV.[32,33] On the basis of these results, we conclude that for the 48 h SAM the dominant intermolecular interactions are H-bonding, although $\pi-\pi$ stacking and dipole−dipole interactions still play a role.

5. Driving Forces behind the Formation of the Wavelike Rows. So far, we have seen that molecules MA, MPAA, MPNAA, and MPCAA all could self-assemble into similar structure of wavelike rows. In the following text, we discuss the possible driving forces for the formation of this fundamental packing structure. Realizing the similarity, surface registry (or adsorption site) is probably the first factor that one may consider. However, because the unit cell size of Au(111) is only 2.88 Å and the distances between available neighboring adsorption sites (such as the fcc, hcp, bridge, and atop sites) are within 1 Å, whereas the size differences along the wavelike structures in the unit cells of these SAMs are about 5 Å or even larger, surface registry should not be the dominant factor. We thus speculate that the structure is favored by the $\pi-\pi$ stacking interactions because they prefer to have a small but nonzero γ. Figure 6 schematically shows that if the parallel-displaced $\pi-\pi$ stacking prefers a specific combination of θ and γ then wavelike $\pi-\pi$ stacking rows can form only if γ is nonzero. In other words, the wavelike $\pi-\pi$ row structure indicates that, at least for large π-systems, parallel-displaced $\pi-\pi$ stacking prefers a nonzero γ.

Obviously, this statement does not conflict with the nature of $\pi-\pi$ interactions[24] but still needs to be confirmed by calculations. In view of the fact that such calculations are still quite difficult,[24,27,28] we seek support from the parallel-displaced $\pi-\pi$ stacking cases involved in proteins and DNA. It turns out that in the case of protein the parallel-displaced $\pi-\pi$ stacking interactions stabilize the tertiary structures and require a nonzero γ.[26] As for DNA, it is well known that the helix is bonded together by hydrogen bonding between the complementary bases and is stabilized by the parallel-displaced $\pi-\pi$ stacking interactions between the base pairs and that the values of θ are around 30°.[24]

Surprisingly, no direct statements pertaining to γ have yet been made. However, we notice that for the most important type of DNA, that is, B-DNA, the base pairs are not perpendicular to the helical axis but have a negative tilted angle of 6°. In addition, the base pairs have a propeller twist angle a bit larger than 10°.[25] These angles lead to γ values of around 10° rather than zero. The data from the well-established structures of both DNA and protein strongly support the idea that the formation of SAMs of aromatic thiols (at least for those with a large π-system) is driven by parallel-displaced $\pi-\pi$ stacking, which prefers a nonzero γ, as consistently shown by our observations of four different molecules. Specifically, for the four SAMs studied in our case, γ angles are all close to 10−12° (<30°) at

(33) Jaffe, R. L.; Smith, G. D. *J. Chem. Phys.* **1996**, *105*, 2786−2788. Sinnokrat, M. O.; Sherrill, C. D. *J. Am. Chem. Soc.* **2004**, *126*, 7690−7697.

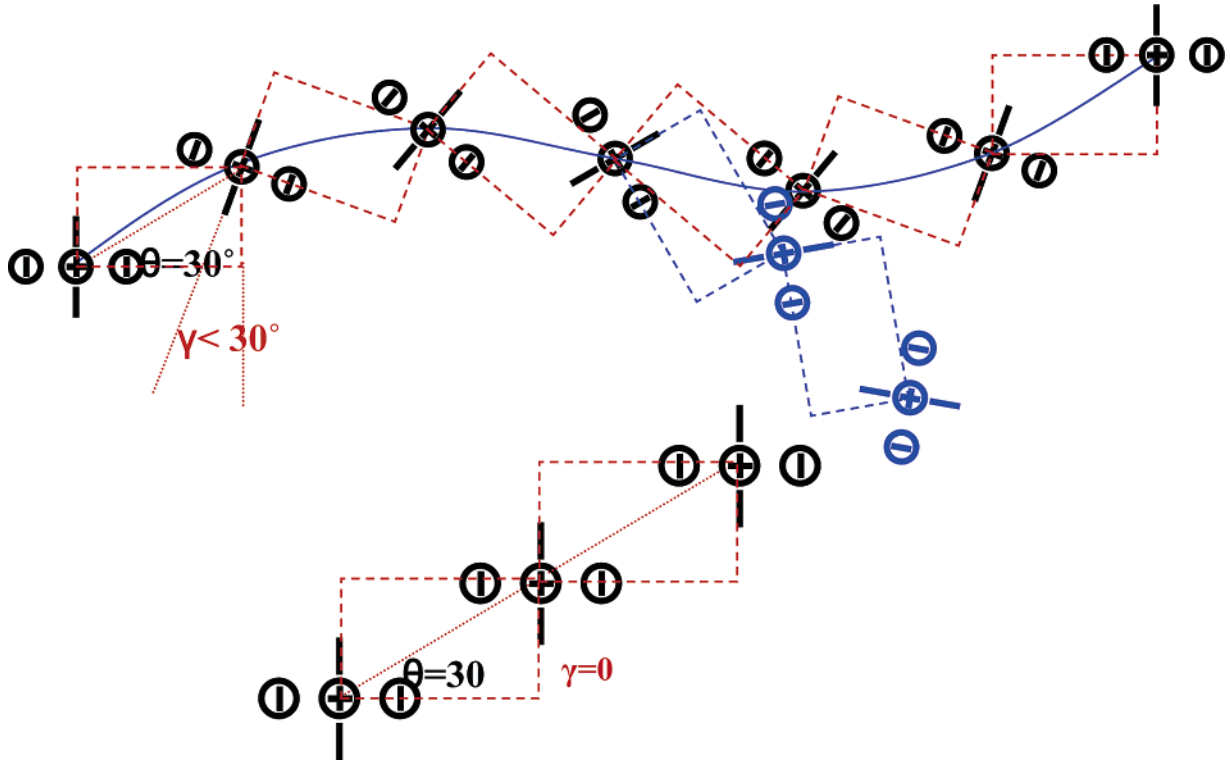

Figure 6. Schematic drawing of the formation of a wavelike molecular row for the anthracene-based molecules showing a nonzero γ at a fixed θ. In contrast, the formation of a straight molecular row at a zero γ combined with a fixed θ is shown in the lower panel.

a fixed θ, which eventually results in the formation of wavelike molecular rows with the four-molecule periodicity for anthracene-based molecules (except for the 48 h SAM of MPCAA), as shown in Figure 6.

Summary

Using STM, we have systematically investigated the SAMs of four specially designed anthracene-based thiols, that is, MA, MPAA, MPNAA, and MPCAA adsorbed on the Au(111) substrate. The results are summarized as follows. (i) In the SAM of MA, the parallel-displaced $\pi-\pi$ stacking interactions are dominant, which aligns the MA molecules into wavelike rows along the $\pi-\pi$ interaction direction. (ii) The MPAA SAM is exceedingly similar to that of MA, but with improved long-range ordering that is obviously due to the enhanced molecular flexibility of the phenyl-acetylene group as a spacer. (iii) The strong parallel-displaced $\pi-\pi$ stacking interactions make such SAM structures very stable so that similar structures are also preserved in the case of MPNAA. The repulsive dipole−dipole interactions are not strong enough to destroy the fundamental structure of the MPNAA SAM. (iv) To our surprise, similar wavelike row structures also persist in the 24 h SAMs of MPCAA, where both intermolecular hydrogen-bonding interactions and repulsive dipole−dipole interactions are involved. (v) Parallel-displaced $\pi-\pi$ stacking interactions, at least for molecules with large π-systems, prefer a small, nonzero γ angle, which leads to the fundamental wavelike row structure in the $\pi-\pi$ stacking direction for all of the molecules studied.

On the basis of these solid findings, we come to the conclusion that the parallel-displaced $\pi-\pi$ stacking interactions, which are well known to stabilize the double helical structures of DNA and the tertiary structures of proteins, are also the most important force in stabilizing aromatic thiol SAMs. From the point of view of applications, these findings are significant, and such SAMs are very promising for nanotechnology and molecular electronics simply because of their high stability against the attachment of a variety of useful functional groups. It is quite encouraging that this conclusion has been receiving support from recent papers.[34,35]

Acknowledgment. The work in Beijing was financially supported by National Science Foundation and the Ministry of Science and Technology (2001CB610500) of China. This work was also supported by two earmarked grants from the Research Grant Council of Hong Kong, with reference numbers 402803 and 401303. Financial support from the Air Force Office of Scientific Research (AFOSR-BIC) and the Army Research Office (ARO-DURINT) is also appreciated.

Supporting Information Available: Detailed methods. This material is available free of charge via the Internet at http://pubs.acs.org.

LA052987U

(34) Zareie, M. H.; Ma, H.; Reed, B. W.; Jen, A. K.-Y.; Sarikaya, M. *Nano Lett.* **2003**, *3*, 139−142.
(35) Kang, S. H.; Ma, H.; Kang, M.-S.; Kim, K.-S.; Jen, A. K.-Y.; Zareie, M. H.; Sarikaya, M. *Angew. Chem., Int. Ed.* **2004**, *43*, 1512−1516.